Impact of future nitrous oxide and carbon dioxide emissions on the stratospheric ozone layer

2015 Environ. Res. Lett. 10 034011

(http://iopscience.iop.org/1748-9326/10/3/034011)

Environmental Research Letters

OPEN ACCESS

RECEIVED
31 December 2014

REVISED
6 February 2015

ACCEPTED FOR PUBLICATION
19 February 2015

PUBLISHED
5 March 2015

LETTER

Impact of future nitrous oxide and carbon dioxide emissions on the stratospheric ozone layer

Richard S Stolarski[1], **Anne R Douglass**[2], **Luke D Oman**[2] **and Darryn W Waugh**[1]

[1] Johns Hopkins University, Baltimore, MD, USA
[2] NASA Goddard Space Flight Center, Greenbelt, MD, USA

E-mail: rstolar1@jhu.edu

Keywords: ozone layer, nitrous oxide, carbon dioxide

Abstract

The atmospheric levels of human-produced chlorocarbons and bromocarbons are projected to make only small contributions to ozone depletion by 2100. Increases in carbon dioxide (CO_2) and nitrous oxide (N_2O) will become increasingly important in determining the future of the ozone layer. N_2O increases lead to increased production of nitrogen oxides (NO_x), contributing to ozone depletion. CO_2 increases cool the stratosphere and affect ozone levels in several ways. Cooling decreases the rate of many photochemical reactions, thus slowing ozone loss rates. Cooling also increases the chemical destruction of nitrogen oxides, thereby moderating the effect of increased N_2O on ozone depletion. The stratospheric ozone level projected for the end of this century therefore depends on future emissions of both CO_2 and N_2O. We use a two-dimensional chemical transport model to explore a wide range of values for the boundary conditions for CO_2 and N_2O, and find that all of the current scenarios for growth of greenhouse gases project the global average ozone to be larger in 2100 than in 1960.

1. Introduction

Anthropogenic ozone-depleting chlorocarbons and bromocarbons are declining due to cessation of their production as a result of the Montreal Protocol and its amendments (Andersen and Sarma 2002). By the year 2100 the role of chlorine and bromine in determining the amount of ozone in the stratosphere will be small, and factors including other trace gases will control the ozone concentration.

One factor that will impact future ozone is the concentration of nitrous oxide (N_2O). Reaction of N_2O with excited atomic oxygen ($O(^1D)$) is the primary natural source of nitrogen oxides ($NO_x = NO + NO_2$) to the stratosphere (McElroy and McConnell 1971). As NO_x make the largest contribution to stratospheric ozone loss, even for elevated chlorine levels (e.g., figure 9.2 of Holloway and Wayne 2010), an increase in N_2O could decrease stratospheric ozone. In fact, Ravishankara *et al* (2009) have shown that N_2O is the dominant ozone depleting substance (ODS) currently emitted, and is expected to remain so through the remainder of the 21st century. Kanter *et al* (2013) have suggested that the ozone impact of N_2O could be used as a basis for international regulations to control its future emissions to the atmosphere.

Another important factor that will impact future ozone levels is the concentration of carbon dioxide (CO_2). CO_2 cools the stratosphere, slowing temperature-dependent ozone loss processes, resulting in rising ozone levels (Brasseur and Hitchman 1988). Model calculations indicate that past and future increases in CO_2 should speed-up the Brewer–Dobson circulation (e.g., Butchart *et al* 2006), which would decrease ozone in the tropics and increase ozone in middle and high latitudes (e.g., Austin and Wilson 2006, Shepherd 2008, Li *et al* 2009). The combination of cooling and the speed-up of the Brewer–Dobson circulation can lead to a 'super-recovery' of ozone at middle and high latitudes to amounts greater than observed in the pre-CFC era (pre-1960).

Cooling also affects ozone loss through its impact on the amount of nitrogen oxides. The NO_x loss reaction ($N + NO \rightarrow N_2 + O$) competes with the reaction of N atoms with O_2 to form NO. The $N + O_2$ reaction is strongly temperature dependent (Sander *et al* 2010). Cooler temperatures favor the loss reaction, thus reducing the effectiveness of N_2O in producing NO_x.

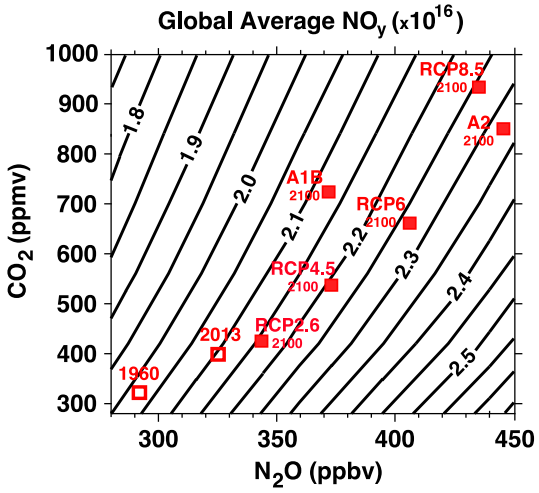

Figure 1. Global area-weighted average NO_y column (in 10^{16} molecules/cm^2) as a function of the N_2O and CO_2 lower boundary conditions assumed in the GSFC 2D model. In all simulations the boundary conditions for chlorine containing species sums to 2 ppbv chlorine, and the boundary condition for methane is held at 1.8 ppmv. Open red squares indicate the model results for 1960 and 2013 conditions. Filled red squares indicate the results for the year 2100 conditions for the SRES and RCP scenarios.

This feedback between temperature and NO_x concentrations affects the impact of increased N_2O on stratospheric ozone. For example, Rosenfield and Douglass (1998) explored the relationship between NO_x and stratospheric cooling, noting that for fixed N_2O boundary conditions the upper stratospheric NO_x decreased by 15% for doubled CO_2.

In recent years, several studies have examined the interactions of changing CO_2 and N_2O on ozone using two-dimensional (Fleming *et al* 2011, Portmann *et al* 2012) or three-dimensional (Oman *et al* 2010, Plumber *et al* 2010, Revell *et al* 2012a, 2012b, Wang *et al* 2014) models. These model studies have shown that CO_2-induced stratospheric cooling and strengthening of the meridional circulation reduces the yield of NO_x from N_2O, and mitigate the effectiveness of N_2O in depleting ozone. Further, for the GHG scenarios considered, changes in NO_x have only a small effect on the future evolution of ozone (e.g., Oman *et al* 2010, Plummer *et al* 2010).

The above studies have focused primarily on ozone changes for a single scenario for future GHG concentrations or have examined only a limited range of N_2O and CO_2 boundary conditions. Here we examine the coupled impacts of changes in N_2O and CO_2 on stratospheric NO_x and ozone for a wide range of future boundary conditions, encompassing the range of values in the year 2100 from the Intergovernmental Panel on Climate Change (IPCC) scenarios. For all of the current scenarios for growth of N_2O and CO_2, the model indicates larger global average column ozone in 2100 than in 1960.

2. Model and simulations

We examine the output from steady-state simulations of stratospheric composition obtained using the two-dimensional Goddard Space Flight Center coupled chemistry–radiation–dynamics model (GSFC2D). Fleming *et al* (2011) describe in detail this model and its performance compared with the three-dimensional Goddard Earth Observing System Chemistry Climate Model (GEOSCCM) (Pawson *et al* 2008). Briefly, we used the model with a 2 km vertical resolution and 10° latitude resolution. Many of the components of the GSFC2D model are the same as those in GEOSCCM. These include: the infrared (IR) radiative transfer scheme (Chou *et al* 2001); the photolytic calculations (Anderson and Lloyd 1990, Jackman *et al* 1996); and the microphysical model for polar stratospheric cloud formation (Considine *et al* 1994).

The dynamics in GSFC2D are coupled to chemistry through the IR heating and UV absorption. Mixing and momentum deposition are computed using a linearized parameterization. The lower boundary condition for the dynamics is solved for planetary zonal wave numbers 1–4 (see Fleming *et al* 2011 for details). The model includes mixing under the assumption that horizontal eddy mixing is directed along the zonal mean isentropes, and projects the K_{yy} mixing rates onto isentropic surfaces. The model also includes parameterized gravity wave breaking that is interactive with the mean flow (Appendix A of Fleming *et al* 2011).

Fleming *et al* (2011) show that the time-dependent ozone responses from GSFC2D and GEOSCCM models are similar for the reference simulation of ODSs and greenhouse gases used in the second phase of the SPARC validation activity for chemistry climate models (CCMVal-2) (SPARC CCMVal 2010). Additional simulations with GSFC2D (Fleming *et al* 2011) exploit its computational efficiency while separating the contributions of the ODSs and other time-varying source gases to ozone response. GSFC2D also produced results consistent with the GEOSCCM in 'world avoided' simulations with unabated increases in anthropogenic chlorocarbons and bromocarbons (Newman *et al* 2009) demonstrating that the responses of both models to large perturbations are consistent. Here we again exploit the computational efficiency of GSFC2D, this time focusing on the relative and combined effects of N_2O and CO_2 on both the radiation and chemistry of the stratosphere.

We examine the sensitivity of both the global amount of total reactive nitrogen (NO_x plus reservoir gases $NO_y = N + NO_x + HNO_3 + ClONO_2 + BrONO_2$) and ozone ($O_3$) by running the GSFC2D model to a steady state for three values of the lower boundary condition for N_2O (280, 360 and 440 ppbv) for each of five values of the lower boundary condition for CO_2 (280, 420, 560, 700 and 840 ppmv). The units for the boundary conditions are parts per

billion by volume (1 ppbv = 10^{-9} moles/mole) and parts per million by volume (1 ppmv = 10^{-6} moles/mole). For each of these simulations, CFC boundary conditions are set to achieve 2 ppbv of Cl_y in the upper stratosphere. This is approximately the amount experienced in 1980 and expected to be reached in 2050. The CH_4 boundary condition is also set at a fixed value (1.8 ppmv) in all simulations.

3. Reactive nitrogen (NO_y)

We first examine how NO_y varies with N_2O and CO_2 boundary conditions. We focus on the globally average total column NO_y ('global NO_y' for short), as a simple metric for the NO_y. Figure 1 presents the global NO_y from the GSFC2D simulations as a function of the N_2O and CO_2 boundary conditions.

Figure 1 shows that the global-average NO_y increases with increasing N_2O and fixed CO_2. The increase in global NO_y is with a near linear function of lower boundary N_2O, but the relative rate of increase of NO_y is less than that of N_2O. For example, there is a 60% increase in N_2O for the range shown in figure 1 (280–450 ppbv) but the increase in NO_y is only around 32% (e.g., 2.0–2.65 ppbv when CO_2 = 300 ppmv). This difference in relative increase is because N_2O is not the only source of atmospheric NO_y. Galactic cosmic rays, lightning, and pollution are also sources of NO_y. These are included in GSFC2D and contribute about a 1/3 of the global NO_y in the model at 320 ppbv N_2O.

For increasing CO_2 with fixed N_2O boundary conditions global NO_y decreases as shown in figure 1. This occurs primarily because increasing CO_2 cools the stratosphere, altering the rate of chemical reactions of the production and loss of NO_y. Increasing CO_2 also speeds up the mean meridional circulation (so called 'Brewer–Dobson circulation') in the model, but this has less net impact on NO_y. The acceleration of the Brewer–Dobson circulation pushes N_2O upward in the tropics, raising the altitude at which N_2O reacts with $O(^1D)$ to produce NO_y and also pushing more NO_y upward into the destruction region (Rosenfield and Douglass 1998).

To better understand the impact of increases in CO_2 on NO_y, we examine the production and loss of NO_y. NO_y is produced mainly from N_2O via the reaction

$$N_2O + O^1D \rightarrow NO + NO \ , \qquad (1)$$

while the NO_y loss rate is controlled by the reaction

$$N + NO \rightarrow N_2 + O. \qquad (2)$$

The N atoms participating in reaction (2) are generated by the photolysis of NO to form N + O. The N atoms have two possible paths; they can react with NO as in reaction (2) to reform N_2 or they can react with O_2 to reform NO with no net loss of NO_y. Presuming steady state for nitrogen atoms, the following expression is obtained for NO_y loss:

$$\text{Loss} = 2k_{N,NO}[N][NO] \approx \frac{2k_{N,NO}J_{NO}[NO]^2}{k_{N,NO}[NO] + k_{N,O_2}[O_2]}, \qquad (3)$$

where square brackets indicate concentrations in molecules/cm^3, $k_{N,NO}$ is the rate coefficient for the reaction of N with NO, $k_{N,O2}$ is the rate coefficient for the reaction of N with O_2, and J_{NO} is the photolysis rate of NO. As the temperature decreases due to the addition of CO_2 and other GHGs the rate coefficient $k_{N,O2}$ decreases, reducing the denominator in equation (3) and increasing the total loss rate for NO_y. Although J_{NO} values are shown to vary widely among the CCMs that participated in CCMVal-2, differences in J_{NO} would affect the magnitude of the loss of NO_y in a given CCM but not the sensitivity of loss to cooling. The relative magnitude of the two terms in the denominator is a function of both the temperature and the amount of NO. At 10 parts per billion by volume (ppbv) of NO and 240 K the N + O_2 term is about 4 times larger than the N + NO term. Thus the change in rate of the N + O_2 reaction caused by cooling almost linearly translates into a change in the loss rate for NO_y. Another way of thinking of this result is that a decrease in temperature favors the reaction branch of N + NO, leading to increased NO_y loss due to this reaction.

To illustrate this, figure 2 shows the variation of the globally-averaged production, loss, and concentration of NO_y for CO_2 increasing from 300 to 850 ppmv (with N_2O boundary condition fixed at 360 ppmv). As CO_2 increases there is a moderate change in the NO_y production but a large increase in its loss, leading to a reduction in the overall NO_y concentration.

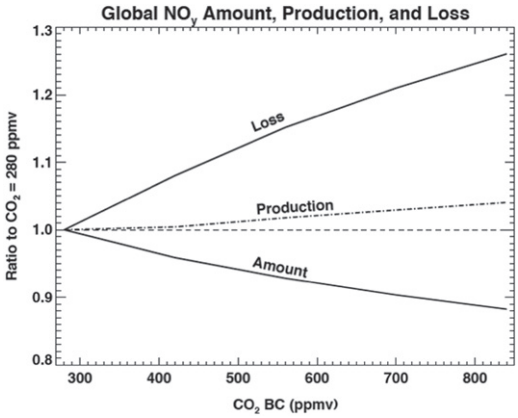

Figure 2. Variation of global-averaged loss, production, and concentration ('amount') of NO_y as a function of the CO_2 lower boundary condition (BC), Results assume a constant N_2O (=360 ppbv) lower boundary condition. The loss term is determined from equation (3) and is not linear in the total NO_y amount.

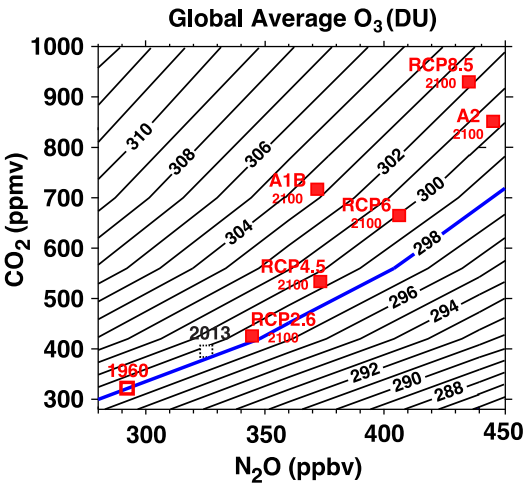

Figure 3. As in figure 3 except for global area-weighted average ozone column (in DU). The dashed square, labeled 2013, is the value that the model would indicate for ozone if the chlorine concentration had been 2 ppbv. The heavy blue line is the 1960 global average column amount of ozone of 298 DU.

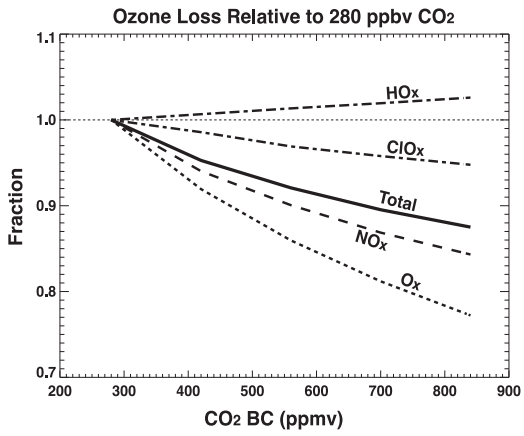

Figure 4. Fraction of globally-averaged ozone loss due to each catalytic loss cycle as a function of the CO_2 boundary condition (BC) in the model simulation. The loss fraction for each cycle has been normalized to its value at 280 ppmv of CO_2. The total is indicated by the heavy black line, showing a decrease to about 88% of its 280 ppmv value when the CO_2 boundary condition reaches 840 ppmv. The fractions for the O_x and NO_x cycles decrease more rapidly than the total because these are the most temperature-sensitive cycles. The fractions for the ClO_x and HO_x cycle decrease less (small increase for HO_x) because these are the least temperature-sensitive cycles.

As increasing N_2O causes global NO_y to increase but increasing CO_2 affects global NO_y in the opposite sense, the change in global NO_y when both N_2O and CO_2 increase depends on their relative increases. As shown in figure 1, for larger increases in CO_2 relative to N_2O there is a decrease in global-average NO_y, whereas there is an increase in global-average NO_y if the relative increase in N_2O is larger.

We now consider the changes in NO_y for changes in N_2O and CO_2 corresponding to the different Special Report on Emissions Scenarios (SRES) (IPCC 2000) or Representative Concentration Pathways (RCPs) (Moss *et al* 2010, Meinshausen *et al* 2011). The red squares in figure 3 show the increases in CO_2 and N_2O following different future scenarios. The open red square in figure 1 is placed at the observed N_2O and CO_2 values in 1960, while the filled red squares are placed at the N_2O and CO_2 values projected for the year 2100 for the SRES A1B and A2 scenarios, and the RCP2.6, RCP4.5, RCP6.0, and RCP8.5 Pathways.

GSFC2D simulates an increase of around 0.1×10^{16} molecules/cm^2 in global NO_y between 1960 and 2100 for the A1B scenario (figure 1), which has been considered in many previous modeling studies. This corresponds to around a 5% increase in global NO_y, which is much less than the 25% increase in the N_2O boundary condition. This small increase in global NO_y for the A1B scenario is consistent with simulations by the three-dimensional CCMs that participated in CCMVal-2. The average change in globally integrated NO_y between 1960 and 2100 for the A1B scenario is $-2\% \pm 5\%$ for the 14 CCMs in CCMVal-2. The change in global-average NO_y is the net effect of the positive and negative regions integrated over the globe (e.g., Oman *et al* 2010), and models with a slightly different balance of NO_y production and loss will get a slightly different answer. The change is small for all models.

For the other IPCC scenarios there are somewhat larger increases in NO_y, but in all cases the percentage increases in global NO_y are much smaller than would be obtained for constant CO_2. The impact of climate (temperature and circulation) change is seen clearly for scenarios with similar N_2O and larger increases in CO_2, i.e., compare RCP4.5 and A1B, A2 with RCP8.5.

4. Ozone (O_3)

We now consider the change in global column amount of ozone from the suite of GSFC2D simulations. Figure 3 shows the global average O_3 as a function of N_2O and CO_2. As for global-average NO_y, the sign of the change in ozone differs between increasing N_2O and increasing CO_2. Global column amount of ozone decreases with increasing N_2O and fixed CO_2, but increases with increasing CO_2 and fixed N_2O. When the increase in CO_2 is large and the N_2O increase is small there is an increase in total ozone, whereas if there is a large N_2O increase and small CO_2 change then there can be a decrease in ozone.

It is important to note that changes in O_3 shown in figure 3 are due not only to changes in NO_x chemistry but also to changes in other ozone loss cycles. In particular, as the stratosphere cools (due to increased CO_2) there is a decrease in the ozone loss via each of the loss cycles. In particular, the O_x and NO_x cycles are strongly temperature dependent while the ClO_x and HO_x cycles are significantly less temperature dependent (see e.g. Stolarski *et al* (2012)). Figure 4 illustrates

the dependence of the contributions of the catalytic cycles as a function of the CO_2 concentration. The importance of the NO_x cycle thus decreases relative to the other cycles as the temperature cools due to CO_2 increases.

As in figure 1, the open red symbol in figure 3 shows the observed values of N_2O and CO_2 in 1960, while the values of N_2O and CO_2 from various scenarios for the year 2100 are indicated by the filled red squares. The simulation using the 1960 concentrations of N_2O and CO_2 (291 and 316 respectively) yielded a global average ozone column of 298 DU as indicated by the open red box and the heavy blue line. For all of the scenarios the global-average ozone in 2100 is greater than that in 1960. The largest increase (5 DU) occurs for A1B, whereas there is only a very small increase for RCP2.6. This 'super-recovery' of column ozone occurs primarily in the mid and high latitudes with little change in the tropics (e.g., Li *et al* 2009).

Caution is required interpreting the results shown in figure 3 as they are from a single model and are for steady state calculations. However, these results are consistent with the 1960 to 2100 transient simulations from GSFC2D and other models. First, the 5.1 DU increase in global ozone from 1960 to 2100 in the GSFC2D model transient A1B simulation (Fleming *et al* 2011) is consistent with the steady-state calculation shown in figure 3. The global ozone difference from 3D CCMs is also of similar magnitude; the multi-model mean increase in ozone for the A1B scenario is 4 ± 2 DU for the 17 CCMs in CCMVal-2 (Eyring *et al* 2010a, 2010b). Furthermore, sensitivity studies from a small subset of CCMs show a similar dependence of global ozone on N_2O and CO_2. For example, the changes in ozone for simulations of the different RCPs vary from slight decrease in global ozone for RCP2.6 to a ~6 DU increase for RCP8.5 (Eyring *et al* 2007), compared to slight increase to ~4 DU increase in figure 3. Revell *et al* (2012b) performed a series of transient simulations with N_2O following the different RCP scenarios but CO_2 and CH_4 following the A1B scenario, and show 2100 global ozone for RCP2.6 ($N_2O = 344$ ppbv) to be 6.7 DU larger than in RCP8.5 ($N_2O = 435$ ppbv). Again, this difference is similar to that in figure 3 (for N_2O increasing from 340 to 445 ppbv with $CO_2 \sim 700$ ppmv). Note that the results for RCP2.6 and RCP8.5 shown in figures 2 and 3 are not directly comparable to the results obtained by other models because our boundary condition for CH_4 is constant (1.8 ppmv). Our results are designed to show the model response for the N_2O/CO_2 relationship without the complicating factor of changes in CH_4. We have run simulations for varying levels of CH_4 and find that global ozone increases by 3–4 DU per ppm of CH_4. The exact amount depends on the amounts of CO_2 and N_2O. For RCP8.5, the CH_4 mixing ratio reaches about 3.5 ppmv by 2100. This results in an extra 6–7 DU of total ozone above the amount shown in figure 3. For RCP2.6, the CH_4 mixing ratio in 2100 is reduced to about 1.2 ppmv resulting in a decrease of 2–3 DU in the deduced total ozone from our model simulations.

5. Conclusions

We performed a series of steady-state simulations with the GSFC2D model to examine the potential future control of the ozone layer, focusing on the year 2100 when the concentrations of chlorine and bromine species will have declined due to the continued implementation of the Montreal Protocol. These simulations show that global-average NO_y and O_3 respond oppositely to increasing N_2O and increasing CO_2. Global NO_y increases and ozone decreases with increasing N_2O and fixed CO_2, whereas NO_y decreases and ozone increases with increasing CO_2 and fixed N_2O. Thus, the responses of NO_y and ozone to increases in N_2O are coupled to increases in CO_2 and climate change.

These simulations indicate that for all of the GHG scenarios considered in recent IPCC assessments there will only be a small change in global NO_y and O_3 for conditions in the year 2100 compared to the year 1960. The GSFC2D models shows small increases in global NO_y for all IPCC scenarios, with the percentage change significantly smaller than the increase in the N_2O mixing ratio imposed at the lower boundary of the model. This occurs because the total amount of NO_x available for catalytic ozone loss depends on the amounts of both N_2O and CO_2 assumed at the lower boundary of the model.

For all scenarios, we also simulate a small increase (~0–5 DU) in global O_3 in 2100 compared to that in 1960 for constant CH_4. This increase occurs mainly because of the projected increases in CO_2 and despite projected increases in N_2O. Taking CH_4 variation into account, we obtain a slight decrease (~2 DU) in global O_3 in 2100 for the RCP2.6 scenario because of the projected decrease in CH_4 in this scenario.

Although N_2O will likely be the most important anthropogenic ODS by the end of the 21st century (Ravishankara *et al* 2009) and decreases in global ozone are to be expected for an N_2O increase at constant CO_2, the simulations presented here suggest that increases in N_2O will only lead to large reductions in global O_3 in the unlikely situation where CO_2 concentrations are held constant while N_2O concentrations continue to grow rapidly.

Acknowledgments

We thank Charles Jackman and Eric Fleming for making the code of the GSFC2D model available for these calculations.

References

Anderson D E and Lloyd S A 1990 Polar twilight UV–visible radiation field: perturbations due to multiple scattering, ozone depletion, stratospheric clouds, and surface albedo *J. Geophys. Res.: Atmos.* (1984–2012) **95** 7429–34

Andersen S O and Sarma K M 2002 *Protecting the Ozone Layer: The United Nations History* (London: Earthscan Publications Ltd)

Austin J and Wilson J R 2006 Ensemble simulatins of the decline and recovery of stratospheric ozone *J. Geophys. Res.* **111** D16314

Brasseur G and Hitchman M H 1988 Stratospheric response to trace gas perturbations—changes in ozone and temperature distributions *Science* **240** 634–7

Butchart N *et al* 2006 Simulations of anthropogenic change in the strength of the Brewer–Dobson circulation *Clim. Dyn.* **27** 727–41

Chou M-D, Suarez M J, Liang X-Z and Yan M-H 2001 A thermal infrared radiation parameterization for atmospheric studies *NASA Tech. Memo. NASA/TM-2001-104606, 9* (Green-Belt, MA: NASA)

Considine D B, Douglass A R and Jackman C H 1994 Effects of a polar stratospheric cloud parameterization on ozone depletion due to stratospheric aircraft in a two-dimensional model *J. Geophys. Res.: Atmos.* (1984–2012) **99** 18879–94

Eyring V *et al* 2007 Multimodel projections of stratospheric ozone in the 21st century *J. Geophys. Res.* **112** D16303

Eyring V *et al* 2010a Sensitivity of 21st century stratospheric ozone to greenhouse gas scenarios *Geophys. Res. Lett.* **37** L16807

Eyring V *et al* 2010b Multi-model assessment of stratospheric ozone return dates and ozone recovery in CCMVal-2 models *Atmos. Chem. Phys.* **10** 9451–75

Fleming E L, Jackman C H, Stolarski R S and Douglass A R 2011 A model study of the impact of source gas changes on the stratosphere for 1850-2100 *Atmos. Chem. Phys.* **11** 8515–41

Holloway A M and Wayne R P 2010 *Atmospheric Chemistry* (London: Royal Society of Chemistry Publishing)

IPCC 2000 Intergovernmental Panel On Climate Change (IPCC) *Special Report on Emissions Scenarios: A Special Report of Working Group III of the Intergovernmental Panel on Climate Change* Rep. pp 599 (Cambridge: Cambridge University Press)

Jackman C H, Fleming E L, Chandra S, Considine D B and Rosenfield J E 1996 Past, present, and future modeled ozone trends with comparisons to observed trends *J. Geophys. Res.* **101** 28753–67

Kanter D, Mauzerall D L, Ravishankara A R, Daniel J S, Portmann R W, Grabiel P M, Moomaw W R and Galloway J N 2013 A post-Kyoto partner: considering the stratospheric ozone régime as a tool to manage nitrous oxide *Proc. Natl Acad. Sci.* **110** 4451–7

Li F, Stolarski R S and Newman P A 2009 Stratospheric ozone in the post-CFC era *Atmos. Chem. Phys.* **9** 2207–13

McElroy M B and McConnell J C 1971 Nitrous oxide: a natural source of stratospheric NO *J. Atmos. Sci.* **28** 1095–8

Meinshausen M *et al* 2011 The RCP greenhouse gas concentrations and their extensions from 1765 to 2300 *Clim. Change* **109** 213–41

Moss R H *et al* 2010 The next generation of scenarios for climate change research and assessment *Nature* **463** 747–56

Newman P A *et al* 2009 What would have happened to the ozone layer if chlorofluorocarbons (CFCs) had not been regulated? *Atmos. Chem. Phys.* **9.6** 2113–28

Oman L D, Waugh D W, Kawa S R, Stolarski R S, Douglass A R and Newman P A 2010 Mechanisms and feedback causing changes in upper stratospheric ozone in the 21st century *J. Geophys. Res.* **115** D05303

Pawson S, Stolarski R S, Douglass A R, Newman P A, Nielsen J E, Frith S M and Gupta M L 2008 Goddard Earth observing system chemistry-climate simulations of stratospheric ozone-temperature coupling between 1950 and 2005 *J. Geophys. Res.* **113** D12103

Plummer D A *et al* 2010 Quantifying the contributions to stratospheric ozone changes from ozone depleting substances and greenhouse gases *Atmos. Chem. Phys.* **10.18** 8803–20

Portmann R, Daniel J and Ravishankara A 2012 Stratospheric ozone depletion due to nitrous oxide: influences of other gases *Phil. Trans. R. Soc.* B **367** 1256–64

Ravishankara A R, Daniel J S and Portmann R W 2009 Nitrous oxide (N_2O): the dominant ozone-depleting substance emitted in the 21st century *Science* **326** 123–5

Revell L, Bodeker G, Huck P, Williamson B and Rozanov E 2012a The sensitivity of stratospheric ozone changes through the 21st century to N_2O and CH_4 *Atmos. Chem. Phys.* **12** 309–11

Revell L, Bodeker G, Smale D, Lehmann R, Huck P, Williamson B, Rozanov E and Struthers H 2012b The effectiveness of N_2O in depleting stratospheric ozone *Geophys. Res. Lett.* **39** 1–6

Rosenfield J E and Douglass A R 1998 Doubled CO_2 effects on NO_y in a coupled 2D model *Geophys. Res. Lett.* **25** 5381–4394

Sander S P *et al* 2010 *Chemical Kinetics and Photochemical Data for Use in Atmospheric Studies Evaluation number* 17, JPL Report 10-6

Shepherd T G 2008 Dynamics, stratospheric ozone and climate change *Atmos.-Ocean* **46** 117–38

SPARC CCMVal 2010 *SPARC Report of the Evaluation of Chemistry-Climate Models* ed V Eyring, T G Shepherd, D W Waugh, SPARC Report No. 5, WCRP-132, WMO/TD-No. 1526

Stolarski R S, Douglass A R, Remsberg E E, Livesey N J and Gille J C 2012 Ozone temperature correlations in the upper stratosphere as a measure of chlorine content *J. Geophys. Res.* **117** D10305

Wang W, Tian W, Dhomse S, Xie F, Shu J and Austin J 2014 Stratospheric ozone depletion from future nitrous oxide increases *Atmos. Chem. Phys.* **14** 12967–82